



Precursor Ion Survival Energies of Protonated N-Glycopeptides and their Weak Dependencies on High Mannose N-Glycan Composition in Collision-Induced Dissociation

Journal:	<i>Analyst</i>
Manuscript ID	AN-ART-05-2018-000830.R1
Article Type:	Paper
Date Submitted by the Author:	20-Jun-2018
Complete List of Authors:	Aboufazeli, Forouzan; University of Nebraska - Lincoln, Department of Chemistry Dodds, Eric; University of Nebraska - Lincoln, Department of Chemistry

1
2
3
4
5
6
7 **PRECURSOR ION SURVIVAL ENERGIES OF PROTONATED N-GLYCOPEPTIDES AND THEIR**
8
9 **WEAK DEPENDENCIES ON HIGH MANNOSE N-GLYCAN COMPOSITION IN**
10
11 **COLLISION-INDUCED DISSOCIATION**
12

13
14
15
16
17 ***Forouzan Aboufazeli and Eric D. Dodds****
18
19

20
21
22
23 Department of Chemistry
24 University of Nebraska - Lincoln
25
26 Lincoln, NE, 68588-0304, USA
27
28
29
30

31
32
33 *Corresponding Author
34
35 Department of Chemistry
36
37 University of Nebraska – Lincoln
38
39 711 Hamilton Hall, Lincoln, NE, 68588-0304, USA
40
41 E-mail: eric.dodds@unl.edu; Telephone: 1.402.472.3592
42
43
44
45
46

47
48 Submitted to *Analyst* for Consideration as a Paper
49

50 03 May 2018

51 Submitted in Revised Form

52
53
54 20 June 2018
55
56
57
58
59
60

ABSTRACT

Fully realizing the capabilities of tandem mass spectrometry (MS/MS) for analysis of glycosylated peptides will require further understanding of the unimolecular dissociation chemistry that dictates their fragmentation pathways. In this context, the overall composition of a given glycopeptide ion is a key characteristic; however, the extent to which the carbohydrate moiety influences the preferred dissociation channels has received relatively little study. Here, the effect of glycan composition on energy-resolved collision-induced dissociation (CID) behavior was studied for a select menu of 30 protonated high mannose type N-linked glycopeptide ions. Groups of analytes which shared a common charge state, polypeptide sequence, and glycosylation site exhibited 50% precursor ion survival energies that varied only slightly as the size and composition of the oligosaccharide was varied. This was found to be true regardless of whether the precursor ion survival energies were normalized for the number of available vibrational degrees of freedom. The practical consequence of this was that a given collision energy brought about highly similar levels of precursor ion depletion and structural information despite systematic variation of the glycan identity. This lack of sensitivity to oligosaccharide composition stands in contrast to other physicochemical properties of glycopeptide ions (*e.g.*, polypeptide composition, charge state, charge carrier) which sharply influence their energy-resolved CID characteristics. On the whole, these findings imply that the deliberate selection of CID energies to bring about a desired range of fragmentation pathways does not necessarily hinge on the nature of the glycan.

KEYWORDS

Glycosylation; glycoproteins; glycopeptides; glycoproteomics; tandem mass spectrometry; energy-resolved collision-induced dissociation.

INTRODUCTION

The ubiquitous, enzymatically-catalyzed, and non-template-driven modification of proteins by carbohydrates is essential to a multitude of fundamental life processes.¹⁻⁴ Consequently, the glycosylation status of proteins has garnered significant attention from the standpoint of human health and disease.⁵⁻⁷ In this context, anomalous modes of protein glycosylation may be predictive or indicative of a given disease state, as well documented in many forms of cancer.⁸⁻¹⁰ Alternatively, defects of protein glycosylation may serve to trigger a given disease state, such as in the various congenital disorders of glycosylation.¹¹⁻¹⁴ Furthermore, while protein-linked oligosaccharides have been widely recognized for some time as focal points of intermolecular recognition,^{15, 16} protein-borne glycans have also become increasingly credited for their roles in biomolecular signaling.^{17, 18} Taken together, these considerations have served to stimulate great interest in the area of biomedical glycoproteomics. Nevertheless, the determination of glycosylation profiles across many proteins in samples of realistic biological complexity lies well outside of the routine, remaining solidly in the purview of specialized research.

Mass spectrometry (MS) provides an already powerful yet still actively maturing methodological platform for probing the structures of glycoproteins.¹⁹⁻²⁴ MS-based glycoprotein characterization is often performed following enzymatic degradation such that the glycan topology, sites of glycosylation, and site heterogeneity can be inferred through analysis of the resultant proteolytic glycopeptides.²⁵⁻²⁸ Although the accurately measured monoisotopic masses of glycopeptides can, in some cases, be used to make putative glycopeptide assignments,^{29, 30} further verification of glycopeptide composition and connectivity are usually carried out based on tandem MS (MS/MS) analyses.^{31, 32} There exist many available modes of ion dissociation for this purpose,³³⁻³⁶ with the majority of these having been extensively applied to the MS/MS analysis of glycopeptides.^{31, 32} This includes methods based on ion-neutral collisions, such as in collision-induced dissociation (CID);^{37, 38} methods based on ion / electron or ion / ion charge recombination, such as electron capture

1
2
3 dissociation (ECD) or electron transfer dissociation (ETD);³⁹⁻⁴⁴ and methods based on
4 absorption of photons, such as infrared multiphoton dissociation (IRMPD) and ultraviolet
5 photodissociation (UVPD).⁴⁵⁻⁵⁰
6
7

8
9 Unsurprisingly, the widely varying energy regimes, activation timescales, and
10 activation mechanisms encompassed by this assortment of MS/MS methods are reflected
11 accordingly in the outcomes of the MS/MS experiments. Indeed, some of these methods
12 have been demonstrated to provide very different coverages of glycopeptide topology
13 relative to one another, providing the opportunity to collect highly orthogonal information by
14 invoking multiple types of MS/MS fragmentation. A particularly potent combination has been
15 that of CID and ETD, which for protonated glycopeptide ions tend to provide information on
16 the oligosaccharide connectivity and polypeptide sequence, respectively.^{31, 32} A number of
17 approaches have been developed to combine these two MS/MS methods such that the
18 advantages of both are afforded for glycopeptide analysis.⁵¹⁻⁵⁵ Nevertheless, any strategy
19 that relies solely on ETD to obtain peptide sequence information is inherently subject to the
20 limitations of ETD, including low precursor ion to fragment ion conversion efficiency for
21 glycopeptides, particularly at lower charge states.^{56, 57}
22
23
24
25
26
27
28
29
30
31
32
33
34

35 The less frequently appreciated capability of CID to yield polypeptide sequence
36 information provides an alternative avenue to the determination of covalent relationships
37 between both monosaccharide and amino acid residues of glycopeptide ions. This is possible
38 because CID is self-complementary in the context of glycopeptide MS/MS analysis, with the
39 type of information garnered depending on the selected collision energy.^{58, 59} This raises the
40 question of whether the optimum MS/MS method for obtaining peptide sequence
41 information (*i.e.*, CID or ETD) depends on the physical and chemical characteristics of the
42 specific glycopeptide ion of interest. In concert, these factors have prompted significant
43 interest in elucidating how the properties of glycopeptide ions that dictate their dissociation
44 channels, and how experimental and instrumental parameters can be tuned to deliberately
45 gather a desired type of glycopeptide structural information.
46
47
48
49
50
51
52
53
54
55
56
57
58
59
60

1
2
3 Motivated by the considerations described above and inspired by previous
4 observations on the ability of CID to capture both peptide sequence and glycan connectivity
5 in a collision energy dependent manner,⁶⁰⁻⁶⁷ we have developed a significant interest in the
6 energy-resolved CID behavior of glycopeptide ions. Previously, we demonstrated that
7 oligosaccharide and polypeptide fragmentation could be accessed for a wide variety of
8 glycopeptide ions, and that alternating between optimum collision energies for each type of
9 scission allowed the collection of aggregate spectra covering most of the glycopeptide
10 connectivity.⁵⁸ An obstacle towards the generalized and automated application of this
11 approach was also realized, in that the collision energies yielding useful information on
12 either the glycan or peptide moieties were strikingly different for the various precursor ions
13 studied. In order to address this issue, we further studied a family of closely related model
14 glycopeptides in which the peptide composition and charge state were varied while holding
15 the identity of the glycan constant. This work revealed that the relative proton mobility^{68, 69}
16 of the various glycopeptides was a decisive factor in determining the collision energies
17 providing glycan connectivity information. By contrast, the collision energies providing
18 peptide fragmentation information exhibited essentially no correlation with the precursor ion
19 proton mobility, but instead were better explained by the proton mobility of intermediate
20 fragmentation products appearing prior to the onset of peptide backbone scission.⁵⁹ We
21 have also compared the energy-resolved CID characteristics of doubly protonated, doubly
22 sodiated, and hybrid protonated sodium adduct glycopeptide ions (all doubly charged)
23 where again the peptide composition and sequence were varied while fixing the identity of
24 the glycan. These studies uncovered marked differences in the stabilities of precursor ions
25 with these different charge carriers, with those involving sodiation having more similar
26 precursor ion survival energies as the amino acid composition and sequence were varied.⁷⁰

51 The present study was undertaken to address one of the parameters that has not
52 been systematically varied in previous studies of glycopeptide energy-resolved CID: namely,
53 the composition and size of the attached glycan. Precursor ion survival curves were
54
55
56
57
58
59
60

1
2
3 measured for an assemblage of protonated glycopeptide ions encompassing four high
4 mannose N-linked oligosaccharide compositions, four peptide backbone sequences, and
5 three charge states. As in previous works, the findings of this study verify the heavy
6 influence of proton mobility (and, relatedly, amino acid composition and ion charge state)
7 on the 50% precursor ion survival energies of protonated glycopeptide ions. Contrastingly,
8 elongation of the N-glycan was not found to have a significant impact on the dissociation
9 thresholds of the same ions. Moreover, when the 50% precursor ion survival energies were
10 normalized for the number of available vibrational degrees of freedom, the influence of the
11 N-glycan size and composition was often further minimized. These findings suggest that, for
12 high mannose N-glycopeptides, the identity of the glycan is not a significant factor in
13 determining the absolute collision energies that lead to a given level of precursor ion
14 depletion, or furnish a given type of structural information. This result is encouraging in the
15 context of large-scale glycoproteomics, as this implies that the identity of the glycan may
16 not play a major role in the rational selection of collision energies for glycopeptide analysis.
17
18
19
20
21
22
23
24
25
26
27
28
29
30
31
32

33 **EXPERIMENTAL**

34
35 ***Glycopeptide Preparation.*** Bovine ribonuclease B (RNase B), urea, dithiothreitol,
36 iodoacetamide, imidazole, formic acid, and trypsin were acquired from Sigma-Aldrich (St.
37 Louis, MO, USA). HPLC grade acetonitrile was purchased from Fisher Scientific (Fair Lawn,
38 NJ, USA). HPLC grade water was obtained from Burdick & Jackson (Muskegon, MI, USA). A
39 solution of $10 \mu\text{g}\cdot\mu\text{L}^{-1}$ of RNase B in 8 M urea and 50 mM NH_4HCO_3 (pH 7.5) was prepared to
40 provide a stock solution of the denatured glycoprotein. Disulfide linkages were reduced by
41 addition of 10 μL of 450 mM dithiothreitol in 50 mM NH_4HCO_3 buffer (pH 7.5) with
42 incubation for 1 h in a 55°C water bath, and the free cysteine side chains were then
43 alkylated by treatment with 10 μL of 500 mM iodoacetamide in 50 mM NH_4HCO_3 (pH 7.5)
44 with incubation in the dark at room temperature. The sample was next diluted with 175 μL
45 of 50 mM NH_4HCO_3 (pH 7.5), mixed thoroughly by vortexing, treated with $0.5 \mu\text{g}\cdot\mu\text{L}^{-1}$
46
47
48
49
50
51
52
53
54
55
56
57
58
59
60

1
2
3 trypsin, and held at 37°C in a gravity convection incubator for 12-16 hours. Next, the
4 volume of the mixture was reduced to approximately 10 μL *via* vacuum centrifugation. The
5 resulting concentrate was reconstituted with 100 μL of 80% CH_3CN / 0.1% HCOOH , and this
6 solution was divided into 20 μL aliquots for further workup. Glycopeptides were purified and
7 enriched from the tryptic digest by solid phase extraction (SPE) using a zwitterionic
8 hydrophilic interaction liquid chromatography (ZIC HILIC) micropipette tips obtained from
9 Protea (Somerset, NJ, USA). SPE was carried out by first conditioning the stationary phase
10 with water, equilibrating with 80% CH_3CN / 0.1% HCOOH , then loading an aliquot of
11 glycopeptide digest. Next, the tip was washed using 80% CH_3CN / 0.1% HCOOH , followed
12 by elution with 0.1% formic acid. In some cases, 10 μL of 10 $\mu\text{g}\cdot\mu\text{L}^{-1}$ imidazole was added
13 to the enriched glycopeptide preparation in order to increase the abundance of lower charge
14 state ions for study.

15
16
17
18
19
20
21
22
23
24
25
26
27 **Tandem Mass Spectrometry.** Corning Pyrex borosilicate capillary tubes with a 1.5
28 - 1.8 mm inner diameter and a length of 100 mm (Corning, NY, USA) were purchased from
29 Fisher Scientific, and were used to fabricate emitters for nanoelectrospray ionization (nESI)
30 with the aid of a vertical micropipette puller. Purified glycopeptide solutions were loaded
31 into the homemade borosilicate emitters and placed in contact with a platinum wire (Alfa
32 Aesar; Ward Hill, MA, USA) that served to apply the potential difference necessary for nESI.
33 All MS/MS experiments were accomplished through the use of a Synapt G2-S HDMS
34 quadrupole time-of-flight (Q-TOF) hybrid mass spectrometer (Waters; Manchester, UK). The
35 nESI capillary voltage was optimized for each experiment, and ranged from 1.0 - 1.5 kV.
36 The trapping region stacked ring ion guide of the instrument was used as the collision cell
37 for MS/MS *via* CID, where argon served as the collision gas at a pressure of approximately
38 $5.0 \cdot 10^{-3}$ mbar. The applied potential difference through which ions were accelerated into
39 the collision cell (ΔU) was varied over the range of 0 - 75 V in 5 V increments to collect
40 energy-resolved CID data.
41
42
43
44
45
46
47
48
49
50
51
52
53
54
55
56
57
58
59
60

1
2
3
4
5
6
7
8
9
10
11
12
13
14
15
16
17
18
19
20
21
22
23
24
25
26
27
28
29
30
31
32
33
34
35
36
37
38
39
40
41
42
43
44
45
46
47
48
49
50
51
52
53
54
55
56
57
58
59
60

Data Handling. MS/MS spectra were acquired and processed using MassLynx 4.1 (Waters). Additional data analysis, processing, and graphing was accomplished using SigmaPlot 10.1 (Systat; Chicago, IL, USA) and IGOR Pro 6.3 (WaveMetrics; Lake Oswego, OR, USA). Integrated peak areas were calculated for precursor and fragment ions appearing in MS/MS spectra using a custom script written and implemented in IGOR Pro 6.3. Fragmentation products resulting from scission of the oligosaccharide were assigned using Domon / Costello nomenclature where possible;⁷¹ however, if a given product ion might have arisen from multiple potential fragmentation pathways (thus rendering the specific Domon / Costello cleavage type ambiguous), compositional assignments were made by indicating the observed monosaccharide loss or losses. In the latter of these conventions, the monosaccharides N-acetylglucosamine and mannose were abbreviated as GlcNAc and Man, respectively. Roepstorff / Fohlmann nomenclature was used to assign fragmentation products resulting from scission of the peptide backbone.⁷² The symbols proposed by Varki *et al.* were used to diagram N-glycan structures.^{73, 74} Underlining was used in order to indicate the site of glycosylation on a given peptide sequence.

RESULTS

Overview. The glycopeptides studied here were generated by tryptic digestion of RNase B, a well characterized model glycoprotein with heterogeneous, high mannose type N-glycosylation at a single site. In addition, the site of glycosylation is flanked by several potential tryptic cleavage sites (*i.e.*, C-terminal of arginine and lysine residues). This facilitates the production of a heterogeneous population of tryptic cleavage products, as steric interference imposed by the oligosaccharide chain decreases the rate of proteolysis at adjacent cleavage sites.⁷⁵⁻⁷⁸ As a result, a combination of fully tryptic and various partially tryptic peptide backbones was generated, providing glycopeptides with amino acid sequences of NLTK, NLTKDR, SRNLTK, and SRNLTKDR. Each of these peptide groups were studied in their glycosylated forms, with the N-oligosaccharides GlcNAc₂Man₅, GlcNAc₂Man₆,

1
2
3 GlcNAc₂Man₇, and GlcNAc₂Man₈. The GlcNAc₂Man₉ glycoform of RNase B was not included in
4 these experiments, as this is the least abundant glycoform and did not yield sufficient ion
5 signal to be studied reproducibly across glycopeptides with different amino acid sequences
6 and charge states. Upon nESI-Q-TOF-MS analysis, each glycopeptide of interest was
7 observed in two charge states, including $z = 1$ (*i.e.*, $M+H$), $z = 2$ (*i.e.*, $[M+2H]^{2+}$), and z
8 $= 3$ (*i.e.*, $M+3H$). The various glycopeptide ions studied here are graphically summarized
9 in **Figure 1**. We note here that the $[NLTK + GlcNAc_2Man_7 + H]^+$ and $[NLTK + GlcNAc_2Man_8$
10 $+ H]^+$ ions were not included in these experiments due to insufficient ion signal for
11 reproducible study.
12
13
14
15
16
17
18
19
20

21 **Precursor Ion Survival Curves.** Each glycopeptide ion targeted for study was
22 quadrupole selected and subjected to CID with a range of collision energies (*i.e.*, ΔU
23 values). In each case, the integrated peak area of the precursor ion was measured relative
24 to the total integrated peak area of the spectrum, expressed as a percentage, and plotted
25 as a function of collision energy. The results shown in **Figure 2** demonstrate that
26 glycopeptides having the same amino acid sequence and charge state (*i.e.*, glycopeptides
27 that differ only in the identity of the glycan) tend to exhibit precursor ion survival curves
28 that are grouped over a relatively narrow range of ΔU values. For example, as illustrated in
29 **Figure 2a**, the doubly protonated ions corresponding to the glycoforms of NLTK exhibit
30 highly overlapping precursor ion survival curves, with all of their 50% depletion points
31 occurring within approximately 1 V of one another. For the same glycopeptides in their
32 singly charged forms, the precursor ion survival curves are shifted to significantly higher
33 collision energies. This is due to two combined effects: **(1)** the singly charged precursor
34 ions are imparted with only half the kinetic energy of their doubly charged counterparts
35 when accelerated through a given potential difference; and **(2)** the proton mobilities^{68, 69} of
36 the NLTK glycoforms are significantly lower for the singly charged precursors as compared
37 to the doubly charged precursors, thus increasing the activation barriers that must be
38 surmounted in order to access charge directed fragmentation mechanisms.⁷⁹ Despite the
39
40
41
42
43
44
45
46
47
48
49
50
51
52
53
54
55
56
57
58
59
60

1
2
3 higher collision energies required to deplete the singly charged precursor ions, their survival
4 curves remained heavily overlapped, reaching 50% depletion within 4 V of one another. This
5 is a rather narrow range in comparison to the shifts in precursor ion survival induced by
6 changes in charge state and proton mobility, which in this example amounted to an
7 approximately 45 V shift in the position of the precursor ion survival curves.
8
9
10
11
12

13 The same measurements were performed for the four high mannose glycoforms of
14 SRNLTK, NLTKDR, and SRNLTKDR in their $[M+2H]^{2+}$ and $[M+3H]^{3+}$ ionic forms (**Figure 2b-**
15 **d**). These energy-resolved CID results reinforce the qualitative conclusions reached in the
16 discussion of **Figure 2a** above, in that the precursor ion survival curves exhibited only
17 modest shifts as a result of increasing the number of mannose residues. By contrast, the
18 dissociation thresholds for the same glycopeptides were subject to much larger shifts with
19 alterations in charge state and proton mobility. Nevertheless, some trending toward
20 increased precursor ion stability was apparent as the number of mannose residues
21 increased. This prompted the question of whether these shifts in precursor ion stability were
22 related to some change in the underlying chemistry of dissociation, or whether this was
23 simply a degrees of freedom effect (*i.e.*, greater stability upon vibrational activation arising
24 from an increase in the number of available normal modes).^{80, 81} This question was
25 addressed by the analyses described in the succeeding section.
26
27
28
29
30
31
32
33
34
35
36
37
38

39 **Precursor Ion Survival Energies.** In order to more quantitatively compare the
40 stabilities of the glycopeptide ions under examination, the collision energies required to
41 achieve half depletion of the precursor ion were determined. This was done by least squares
42 fitting of the approximately linear portions of the precursor ion survival curves presented in
43 **Figure 2**, and subsequent calculation of the collision energies that brought about precursor
44 ion survivals of 50% (ΔU_{50}). The corresponding initial ion kinetic energies that resulted in
45 50% precursor ion survivals (E_{K50}) were then calculated according to **Equation 1**, where z
46 represents the integer charge state of the ion:
47
48
49
50
51
52
53
54
55
56
57
58
59
60

$$E_{k50} = z\Delta U_{50} \quad \text{Equation 1}$$

The number of vibrational degrees of freedom (f_v) was also calculated for each glycopeptide of interest using **Equation 2**, where n indicates the number of atoms:

$$f_v = 3n - 6 \quad \text{Equation 2}$$

Finally, the E_{k50} and f_v values were used to calculate the degrees of freedom normalized 50% precursor ion survival energy (E_{n50}), as provided by **Equation 3**:

$$E_{n50} = \frac{10^3 E_{k50}}{f_v} = \frac{10^3 z \Delta U_{50}}{3n - 6} \quad \text{Equation 3}$$

This relation includes a factor of 10^3 so that the E_{n50} values scale conveniently for comparison to the corresponding ΔU_{50} values. Conceptually, E_{n50} represents the initial precursor ion kinetic energy per vibrational mode which reduced the initial precursor ion population to one-half of the total integrated peak area of the CID spectrum. Because this metric accounts for the number of vibrational modes, differences in precursor ion stability arising from the so-called "degrees of freedom effect" are effectively compensated for.^{80, 81} All relevant f_v , ΔU_{50} , E_{k50} , and E_{n50} values have been provided in **Table S1** of the **Electronic Supplementary Information**.

A comparison of E_{k50} and E_{n50} values for the glycopeptide ions under study is presented in **Figure 3**. Overall, the 50% precursor ion survival energies exhibited only a weak dependence on the composition of the N-glycan when varied from GlcNAc₂Man₅ to GlcNAc₂Man₈. This was found to be the case regardless of whether these energies were normalized for the available degrees of vibrational freedom. When the glycan composition was varied while holding the polypeptide sequence and charge state constant, the E_{n50} values were generally found to occupy a comparable or narrower range of values as compared to the E_{k50} values. For example, as seen in **Figure 3d**, the E_{k50} values for the

1
2
3 [SRNLTKDR + GlcNAc₂Man₅₋₈ + 2H]²⁺ glycopeptides ranged from 80.6 ± 0.8 to 95.8 ± 0.9
4 (a change of about 19%), with the values steadily increasing as with the addition of each
5 successive mannose residue. Meanwhile, the E_{n50} values for the same glycopeptide ions
6 ranged from 87.7 ± 0.8 to 92.4 ± 1.2 (a change of about 5%) and exhibited no clear
7 dependence on the number of mannose residues. This general behavior was also observed
8 for other groups of glycopeptides, which followed qualitatively similar relationships between
9 glycan composition and precursor ion survival energies (e.g., **Figure 3b** for the $z = 3$ ions;
10 **Figure 3c** for the $z = 2$ and $z = 3$ ions). In other cases, addition of mannose residues was
11 found to bring about small decreases in E_{n50} values despite concomitant increases in the E_{k50}
12 metric (e.g., **Figure 3a** for the $z = 1$ and $z = 2$ ions; **Figure 3b** for the $z = 2$ ions; **Figure**
13 **3d** for the $z = 3$ ions). In all cases, changes in the composition of the attached high
14 mannose N-glycan had only a modest impact on the precursor ion stabilities when compared
15 to the far more influential characteristics of charge state and amino acid composition.
16
17
18
19
20
21
22
23
24
25
26
27
28

29 **Assessment of Collision Energy Matched Spectra.** A comparison of the
30 dissociation spectra for the various GlcNAc₂Man₅ and GlcNAc₂Man₈ glycopeptides was next
31 conducted with the collision energies held constant for these two glycoforms of each peptide
32 under examination. In this way, the structural information provided on each analyte could
33 be evaluated for cases in which no attempt was made to adjust CID conditions according to
34 the size of the N-glycan borne by the glycopeptide. In **Figure 4**, the collision energy
35 matched CID spectra for the doubly protonated NLTK glycoforms and the triply protonated
36 SRNLTK, NLTKDR, and SRNLTKDR glycoforms are plotted with the spectra for the
37 GlcNAc₂Man₅ glycopeptides shown as upright traces and the GlcNAc₂Man₈ glycopeptides
38 shown as inverted traces for comparison. In each case, the collision energies were selected
39 to provide CID spectra that had the qualitative appearance of containing numerous
40 structurally informative fragment ions; nevertheless, as noted above, each pairwise
41 comparison of the two glycoforms was conducted at the same ΔU . In general, these
42 fragmentation spectra were dominated by Y-type cleavages of the N-glycan, leading to an
43
44
45
46
47
48
49
50
51
52
53
54
55
56
57
58
59
60

1
2
3 assortment of [M-Man_i] product ions and ultimately resulting in loss of all mannose
4 residues. In each case, the Y₁ ion was also prominently observed. In some cases, additional
5 dissociation pathways were noted, including B-type fragmentation oligosaccharide as
6 evidenced by the presence of oxonium ions (e.g., the [Man₂]⁺ ion seen in **Figures 4a,c**)
7 and scission of the peptide backbone (e.g., the y₂ and b₅ cleavages seen in **Figure 4b**).
8 Strikingly, the fragment ions produced yielded by each glycoform at the same collision
9 energy were heavily overlapped, yielding essentially the same compositional and structural
10 information. In fact, the only ions not appearing in the spectra of both glycoforms were the
11 residual precursor ion, if present, and the larger monosaccharide loss fragments possible for
12 the GlcNAc₂Man₈ ions, and GlcNAc₂Man₅ ions. As shown in **Figure 5**, the same qualitative
13 behavior, characterized by heavily overlapped fragmentation spectra for glycoforms, was
14 also observed when the comparisons were repeated with all ΔU values being increased by
15 15 V. In these more energetic CID experiments, distinctly different fragment ion populations
16 were observed. These dissociation products tended to include increased representation of
17 peptide backbone cleavages (as seen in all the examples presented in **Figures 5a-d**) as
18 well as cross-ring cleavage of the N-glycan (e.g., the ^{0,2}X₀ fragments seen in **Figures**
19 **5a,b,d**). Nevertheless, these collision energy matched spectra remained remarkably similar
20 in terms of the fragment ions yielded and the information they provided. This illustrates that
21 the high correlation between the CID spectra of GlcNAc₂Man₅ and GlcNAc₂Man₈ glycoforms is
22 not unique to a certain set of CID conditions but exists over a significant range of ΔU
23 values, including those corresponding to quite different levels of precursor ion depletion. On
24 the whole, these findings are consistent with the previous results focused on precursor ion
25 stability, suggesting that changes to the number of mannose residues has practically no
26 effect the information content of the resulting CID spectra when acquired at the same
27 collision energies.
28
29
30
31
32
33
34
35
36
37
38
39
40
41
42
43
44
45
46
47
48
49
50
51
52

53 54 55 56 **CONCLUSIONS** 57 58 59 60

1
2
3 Measurement of precursor ion survival curves and 50% precursor ion survival
4 energies was performed *via* low-energy beam-type CID for 30 protonated glycopeptide ions
5 spanning four peptide sequences, four high mannose N-glycan compositions, and three
6 charge states. The data acquired demonstrate that the precursor ion stabilities are heavily
7 dependent upon charge state and peptide composition, as observed in previous studies.
8 Contrastingly, the size and composition of the glycan moiety has a weak to negligible
9 influence on the precursor ion stabilities, regardless of whether the available degrees of
10 vibrational freedom are accounted for. It also appears that any minor differences in
11 precursor ion survival are primarily due to the differing availability of vibrational degrees of
12 freedom, and not related to any changes in the dissociation chemistry at hand. In paired
13 spectra of GlcNAc₂Man₅ and GlcNAc₂Man₈ glycoforms, highly correlated spectra were
14 observed when the peptide group, charge state, and collision energy were held constant.
15 The fragments that were detected afforded highly concordant information on the
16 composition and connectivity of the oligosaccharide group and the polypeptide chain,
17 despite the fact that the same collision energy was used to probe the different high
18 mannose glycoforms. The finding that glycan size and composition exerted only a minor
19 influence over glycopeptide precursor ion stability and the information content of the
20 corresponding CID spectra is a potentially simplifying factor for the acquisition of
21 informative MS/MS data for N-linked glycopeptides. This introduces the possibility that
22 many glycoforms of the same peptide could be optimally probed by CID under the same
23 MS/MS conditions, thus removing one variable from a complex set of considerations where
24 the fragmentation of glycopeptides is concerned. Indeed, the ability to obtain comparable
25 structural information for closely related N-glycoforms without the need to modulate CID
26 collision energy may prove to be a significant observation from the standpoint for
27 automated, online glycoproteomic analyses. Overall, we believe that these findings have
28 implications of considerable breadth for glycoproteomic analysis, as CID is, by a great
29 margin, the most widely available MS/MS method. Future research in this area should
30
31
32
33
34
35
36
37
38
39
40
41
42
43
44
45
46
47
48
49
50
51
52
53
54
55
56
57
58
59
60

1
2
3 include an investigation of whether these observations are generalizable to N-glycopeptides
4 of different classes (e.g., those harboring complex type and hybrid type glycans) and
5 incorporating additional monosaccharides (e.g., fucose and sialic acid residues).
6
7
8
9
10
11
12
13
14

15 **ACKNOWLEDGEMENTS**

16
17 The authors wish to convey their sincere thanks to Venkata Kolli and Yuting Huang
18 for helpful comments on a draft of the manuscript. This work was supported in part by
19 funding from the National Science Foundation, Division of Chemistry, through the Chemical
20 Measurement and Imaging Program (Grant Number 1507989). Support from the University
21 of Nebraska - Lincoln, including funds from the Center for Integrated Biomolecular
22 Communication Research Cluster Development Grant, are also acknowledged.
23
24
25
26
27
28
29
30

31 **ELECTRONIC SUPPLEMENTARY INFORMATION**

32
33 Electronic supplementary information available: Compositions, charge states (z),
34 degrees of freedom (f_v), and 50% precursor ion survival data (ΔU_{50} , E_{k50} , and E_{n50}) for all
35 glycopeptide ions studied.
36
37
38
39
40
41
42
43
44
45
46
47
48
49
50
51
52
53
54
55
56
57
58
59
60

REFERENCES

1. A. Varki, *Glycobiology*, 1993, **3**, 97-130.
2. R. A. Dwek, *Chem. Rev.*, 1996, **96**, 683-720.
3. R. G. Spiro, *Glycobiology*, 2002, **12**, 43R-56R.
4. E. Weerapana and B. Imperiali, *Glycobiology*, 2006, **16**, 91R-101R.
5. K. Ohtsubo and J. D. Marth, *Cell*, 2006, **126**, 855-867.
6. H. J. An, S. R. Kronewitter, M. L. A. de Leoz and C. B. Lebrilla, *Curr. Opin. Chem. Biol.*, 2009, **13**, 601-607.
7. K. N. Schumacher and E. D. Dodds, *Glycoconj. J.*, 2016, **33**, 377-385.
8. B. Adamczyk, T. Tharmalingam and P. M. Rudd, *Biochim. Biophys. Acta*, 2012, **1820**, 1347-1353.
9. M. N. Christiansen, J. Chik, L. Lee, M. Anugraham, J. L. Abrahams and N. H. Packer, *Proteomics*, 2014, **14**, 525-546.
10. S. R. Stowell, T. Ju and R. D. Cummings, *Annu. Rev. Pathol. Mech. Dis.*, 2015, **10**, 473-510.
11. E. Marklova and Z. Albahri, *Clin. Chim. Acta*, 2007, **385**, 6-20.
12. H. Schachter and H. H. Freeze, *Biochim. Biophys. Acta*, 2009, **1792**, 925-930.
13. L. Sturiale, R. Barone and D. Garozzo, *J. Inherit. Metab. Dis.*, 2011, **34**, 891-899.
14. H. H. Freeze, *J. Biol. Chem.*, 2013, **288**, 6936-6945.
15. P. M. Rudd and R. A. Dwek, *Crit. Rev. Biochem. Mol. Biol.*, 1997, **32**, 1-100.
16. L. S. C. Kreisman and B. A. Cobb, *Glycobiology*, 2012, **22**, 1019-1030.

- 1
- 2
- 3 17. Y. Y. Zhao, M. Takahashi, J. G. Gu, E. Miyoshi, A. Matsumoto, S. Kitazume and N.
- 4
- 5 Taniguchi, *Cancer Sci.*, 2008, **99**, 1304-1310.
- 6
- 7 18. G. W. Hart, C. Slawson, G. Ramirez-Correa and O. Lagerlof, *Annu. Rev. Biochem.*,
- 8
- 9 2011, **80**, 825-858.
- 10
- 11 19. W. Morelle, K. Canis, F. Chirat, V. Faid and J. C. Michalski, *Proteomics*, 2006, **6**,
- 12
- 13 3993-4015.
- 14
- 15 20. W. Morelle and J. C. Michalski, *Nat. Protoc.*, 2007, **2**, 1585-1602.
- 16
- 17 21. J. E. Schiel, *Anal. Bioanal. Chem.*, 2012, **404**, 1141-1149.
- 18
- 19 22. W. R. Alley, Jr., B. F. Mann and M. V. Novotny, *Chem. Rev.*, 2013, **113**, 2668-2732.
- 20
- 21 23. M. V. Novotny and W. R. Alley Jr, *Curr. Opin. Chem. Biol.*, 2013, **17**, 832-840.
- 22
- 23 24. S. Gaunitz, G. Nagy, N. L. B. Pohl and M. V. Novotny, *Anal. Chem.*, 2017, **89**, 389-
- 24
- 25 413.
- 26
- 27 25. D. S. Dalpathado and H. Desaire, *Analyst*, 2008, **133**, 731-738.
- 28
- 29 26. H. J. An, J. W. Froehlich and C. B. Lebrilla, *Curr. Opin. Chem. Biol.*, 2009, **13**, 421-
- 30
- 31 426.
- 32
- 33 27. H. Desaire, *Mol. Cell. Proteomics*, 2013, **12**, 893-901.
- 34
- 35 28. V. Kolli, K. N. Schumacher and E. D. Dodds, *Bioanalysis*, 2015, **7**, 113-131.
- 36
- 37 29. H. Desaire and D. Hua, *Int. J. Mass Spectrom.*, 2009, **287**, 21-26.
- 38
- 39 30. J. W. Froehlich, E. D. Dodds, M. Wilhelm, O. Serang, J. A. Steen and R. S. Lee, *Mol.*
- 40
- 41 *Cell. Proteomics*, 2013, **12**, 1017-1025.
- 42
- 43 31. M. Wührer, M. I. Catalina, A. M. Deelder and C. H. Hokke, *J. Chromatogr. B*, 2007,
- 44
- 45 **849**, 115-128.
- 46
- 47 32. E. D. Dodds, *Mass Spectrom. Rev.*, 2012, **31**, 666-682.
- 48
- 49 33. R. A. Zubarev, A. R. Zubarev and M. M. Savitski, *J. Am. Soc. Mass Spectrom.*, 2008,
- 50
- 51 **19**, 753-761.
- 52
- 53 34. J. J. Coon, *Anal. Chem.*, 2009, **81**, 3208-3215.
- 54
- 55 35. S. A. McLuckey and M. Mentivona, *J. Am. Soc. Mass Spectrom.*, 2011, **22**, 3-12.
- 56
- 57
- 58
- 59
- 60

- 1
- 2
- 3 36. D. Rathore, F. Aboufazeli, Y. Huang, V. Kolli, G. S. Fernando and E. D. Dodds,
- 4 *Encycl. Anal. Chem.*, 2015, 1-26.
- 5
- 6
- 7 37. M. Tajiri, M. Kadoya and Y. Wada, *J. Proteome Res.*, 2009, **8**, 688-693.
- 8
- 9 38. K. Vekey, O. Ozohanics, E. Toth, A. Jeko, A. Revesz, J. Krenyacz and L. Drahos, *Int.*
- 10 *J. Mass Spectrom.*, 2013, **345-347**, 71-79.
- 11
- 12
- 13 39. E. Mirgorodskaya, P. Roepstorff and R. A. Zubarev, *Anal. Chem.*, 1999, **71**, 4431-
- 14 4436.
- 15
- 16
- 17 40. K. Hakansson, H. J. Cooper, M. R. Emmett, C. E. Costello, A. G. Marshall and C. L.
- 18 Nilsson, *Anal. Chem.*, 2001, **73**, 4530-4536.
- 19
- 20
- 21 41. N. Manri, H. Satake, A. Kaneko, A. Hirabayashi, T. Baba and T. Sakamoto, *Anal.*
- 22 *Chem.*, 2013, **85**, 2056-2063.
- 23
- 24
- 25 42. J. M. Hogan, S. J. Pitteri, P. A. Chrisman and S. A. McLuckey, *J. Proteome Res.*,
- 26 2005, **4**, 628-632.
- 27
- 28
- 29 43. M. I. Catalina, C. A. Koeleman, A. M. Deelder and M. Wührer, *Rapid Commun. Mass*
- 30 *Spectrom.*, 2007, **21**, 1053-1061.
- 31
- 32
- 33 44. J. P. Williams, S. Pringle, K. Richardson, L. Gethings, J. P. C. Vissers, M. De Cecco, S.
- 34 Houel, A. B. Chakraborty, Y. Q. Yu, W. Chen and J. M. Brown, *Rapid Commun. Mass*
- 35 *Spectrom.*, 2013, **27**, 2383-2390.
- 36
- 37
- 38
- 39 45. J. T. Adamson and K. Hakansson, *J. Proteome Res.*, 2006, **5**, 493-501.
- 40
- 41 46. R. R. Seipert, E. D. Dodds, B. H. Clowers, S. M. Beecroft, J. B. German and C. B.
- 42 Lebrilla, *Anal. Chem.*, 2008, **80**, 3684-3692.
- 43
- 44
- 45 47. R. R. Seipert, E. D. Dodds and C. B. Lebrilla, *J. Proteome Res.*, 2009, **8**, 493-501.
- 46
- 47
- 48 48. L. Zhang and J. P. Reilly, *J. Proteome Res.*, 2008, **8**, 734-742.
- 49
- 50 49. J. A. Madsen, B. J. Ko, H. Xu, J. A. Iwashkiw, S. A. Robotham, J. B. Shaw, M. F.
- 51 Feldman and J. S. Brodbelt, *Anal. Chem.*, 2013, **85**, 9253-9261.
- 52
- 53 50. B. J. Ko and J. S. Brodbelt, *Int. J. Mass Spectrom.*, 2015, **377**, 385-392.
- 54
- 55 51. H. Han, Y. Xia, M. Yang and S. A. McLuckey, *Anal. Chem.*, 2008, **80**, 3492-3497.
- 56
- 57
- 58
- 59
- 60

- 1
2
3 52. I. Perdivara, R. Petrovich, B. Allinquant, L. J. Deterding, K. B. Tomer and M.
4 Przybylski, *J. Proteome Res.*, 2009, **8**, 631-642.
5
6
7 53. Z. Darula, R. J. Chalkley, P. Baker, A. L. Burlingame and K. F. Medzihradszky, *Eur. J.*
8 *Mass Spectrom.*, 2010, **16**, 421-428.
9
10
11 54. C. Singh, C. G. Zampronio, A. J. Creese and H. J. Cooper, *J. Proteome Res.*, 2012,
12 **11**, 4517-4525.
13
14
15 55. V. Kolli, K. N. Schumacher and E. D. Dodds, *Analyst*, 2017, **142**, 4691-4702.
16
17 56. W. R. Alley, Jr., Y. Mechref and M. V. Novotny, *Rapid Commun. Mass Spectrom.*,
18 2009, **23**, 161-170.
19
20
21 57. Z. Zhu, D. Hua, D. F. Clark, E. P. Go and H. Desaire, *Anal. Chem.*, 2013, **85**, 5023-
22 5032.
23
24
25 58. V. Kolli and E. D. Dodds, *Analyst*, 2014, **139**, 2144-2153.
26
27 59. V. Kolli, H. A. Roth, G. De La Cruz, G. S. Fernando and E. D. Dodds, *Anal. Chim.*
28 *Acta*, 2015, **896**, 85-92.
29
30
31 60. O. Krokhin, W. Ens, K. G. Standing, J. Wilkins and H. Perreault, *Rapid Commun.*
32 *Mass Spectrom.*, 2004, **18**, 2020-2030.
33
34
35 61. N. V. Bykova, C. Rampitsch, O. Krokhin, K. G. Standing and W. Ens, *Anal. Chem.*,
36 2006, **78**, 1093-1103.
37
38
39 62. C. W. Damen, W. Chen, A. B. Chakraborty, M. van Oosterhout, J. R. Mazzeo, J. C.
40 Gebler, J. H. Schellens, H. Rosing and J. H. Beijnen, *J. Am. Soc. Mass Spectrom.*,
41 2009, **20**, 2021-2033.
42
43
44
45 63. Z. M. Segu and Y. Mechref, *Rapid Commun. Mass Spectrom.*, 2010, **24**, 1217-1225.
46
47
48 64. N. E. Scott, B. L. Parker, A. M. Connolly, J. Paulech, A. V. G. Edwards, B. Crossett, L.
49 Falconer, D. Kolarich, S. P. Djordjevic, P. Hojrup, N. H. Packer, M. R. Larsen and S. J.
50 Cordwell, *Mol. Cell. Proteomics*, 2011, **10**, 1-18.
51
52
53 65. Q. Cao, X. Zhao, Q. Zhao, X. Lv, C. Ma, X. Li, Y. Zhao, B. Peng, W. Ying and X. Qian,
54 *Anal. Chem.*, 2014, **86**, 6804-6811.
55
56
57
58
59
60

- 1
2
3 66. H. Hinneburg, K. Stavenhagen, U. Schweiger-Hufnagel, S. Pengelley, W. Jabs, P. H.
4 Seeberger, D. V. Silva, M. Wuhrer and D. Kolarich, *J. Am. Soc. Mass Spectrom.*,
5 2016, **27**, 507-519.
6
7
8
9 67. J. Nilsson, *Glycoconj. J.*, 2016, **33**, 261-272.
10
11 68. A. R. Dongre, J. L. Jones, A. Somogyi and V. H. Wysocki, *J. Am. Chem. Soc.*, 1996,
12 **118**, 8365-8374.
13
14
15 69. V. H. Wysocki, G. Tsaprailis, L. L. Smith and L. A. Breci, *J. Mass Spectrom.*, 2000,
16 **35**, 1399-1406.
17
18
19 70. F. Aboufazeli, V. Kolli and E. D. Dodds, *J. Am. Soc. Mass Spectrom.*, 2015, **26**, 587-
20 595.
21
22
23 71. B. Domon and C. E. Costello, *Glycoconj. J.*, 1988, **5**, 397-409.
24
25 72. P. Roepstorff and J. Fohlman, *Biomed. Mass Spectrom.*, 1984, **11**, 601.
26
27 73. A. Varki, R. D. Cummings, J. D. Esko, H. H. Freeze, P. Stanley, J. D. Marth, C. R.
28 Bertozzi, G. W. Hart and M. E. Etzler, *Proteomics*, 2009, **9**, 5398-5399.
29
30
31 74. A. Varki, R. D. Cummings, M. Aebi, N. H. Packer, P. H. Seeberger, J. D. Esko, P.
32 Stanley, G. Hart, A. Darvill, T. Kinoshita, J. J. Prestegard, R. L. Schnaar, H. H.
33 Freeze, J. D. Marth, C. R. Bertozzi, M. E. Etzler, M. Frank, J. F. G. Vliegthart, T.
34 Lütteke, S. Perez, E. Bolton, P. Rudd, J. Paulson, M. Kanehisa, P. Toukach, K. F.
35 Aoki-Kinoshita, A. Dell, H. Narimatsu, W. York, N. Taniguchi and S. Kornfeld,
36 *Glycobiology*, 2015, **25**, 1323-1324.
37
38
39
40
41
42
43 75. P. Juhasz and S. A. Martin, *Int. J. Mass Spectrom.*, 1997, **169**, 217-230.
44
45 76. H. J. An, T. R. Peavy, J. L. Hedrick and C. B. Lebrilla, *Anal. Chem.*, 2003, **75**, 5628-
46 5637.
47
48
49 77. B. H. Clowers, E. D. Dodds, R. R. Seipert and C. B. Lebrilla, *J. Proteome Res.*, 2007,
50 **6**, 4032-4040.
51
52
53 78. E. D. Dodds, R. R. Seipert, B. H. Clowers, J. B. German and C. B. Lebrilla, *J.*
54 *Proteome Res.*, 2009, **8**, 502-512.
55
56
57
58
59
60

- 1
2
3 79. B. Paizs and S. Suhai, *Mass Spectrom. Rev.*, 2005, **24**, 508-548.
4
5 80. S. Indelicato, D. Bongiorno, S. Indelicato, L. Drahos, V. Turco Liveri, L. Turiak, K.
6
7 Vekey and L. Ceraulo, *J. Mass Spectrom.*, 2013, **48**, 379-383.
8
9 81. A. Memboeuf, A. Nasioudis, S. Indelicato, F. Pollreisz, A. Kuki, S. Keki, O. F. van den
10
11 Brink, K. Vekey and L. Drahos, *Anal. Chem.*, 2010, **82**, 2294-2302.
12
13
14
15
16
17
18
19
20
21
22
23
24
25
26
27
28
29
30
31
32
33
34
35
36
37
38
39
40
41
42
43
44
45
46
47
48
49
50
51
52
53
54
55
56
57
58
59
60

FIGURES AND CAPTIONS

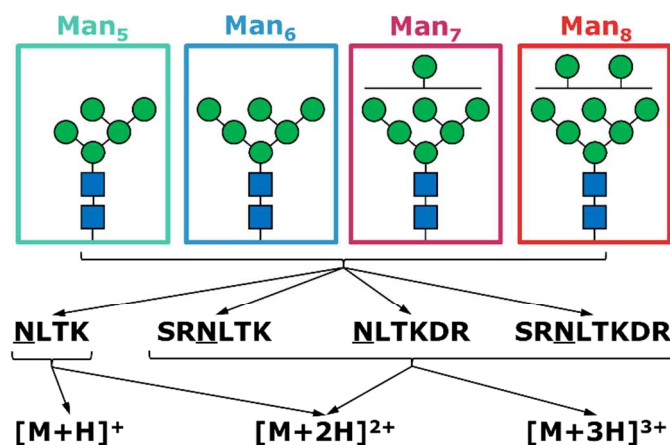


Figure 1. Illustrated summary of the protonated high mannose N-linked glycopeptide ions studied here. The suite of analytes encompassed N-glycans with the compositions GlcNAc₂Man₅, GlcNAc₂Man₆, GlcNAc₂Man₇, and GlcNAc₂Man₈; peptides with the sequences NLTK, SRNLTK, NLTKDR, and SRNLTKDR; and charge states ranging from $z = +1$ to $z = +3$.

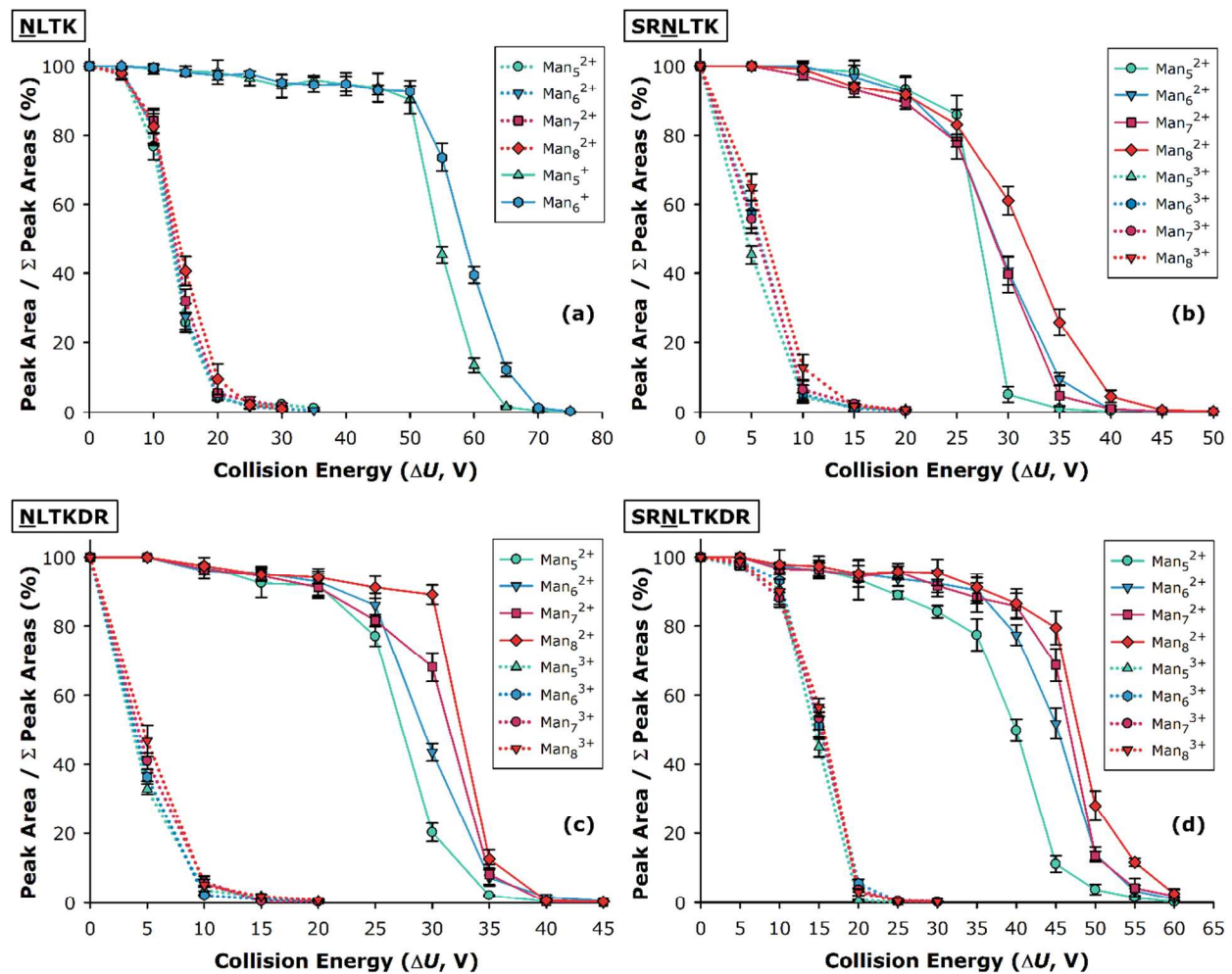


Figure 2. Precursor ion survival curves for glycopeptides with the peptide sequences NLTK (a), SRNLTK (b), NLTKDR (c), and SRNLTKDR (d), harboring N-linked glycans with the compositions $\text{GlcNAc}_2\text{Man}_5$, $\text{GlcNAc}_2\text{Man}_6$, $\text{GlcNAc}_2\text{Man}_7$, and $\text{GlcNAc}_2\text{Man}_8$. Two charge states were considered in each case: $z = 1$ and $z = 2$ in (a); $z = 2$ and $z = 3$ in (b - d). Error bars represent the standard deviation of four replicate determinations arising from separate acquisitions. Data for the $[\text{NLTK} + \text{GlcNAc}_2\text{Man}_7 + \text{H}]^+$ and $[\text{NLTK} + \text{GlcNAc}_2\text{Man}_8 + \text{H}]^+$ ions are not shown in (a) due to insufficient ion signal for reproducible study.

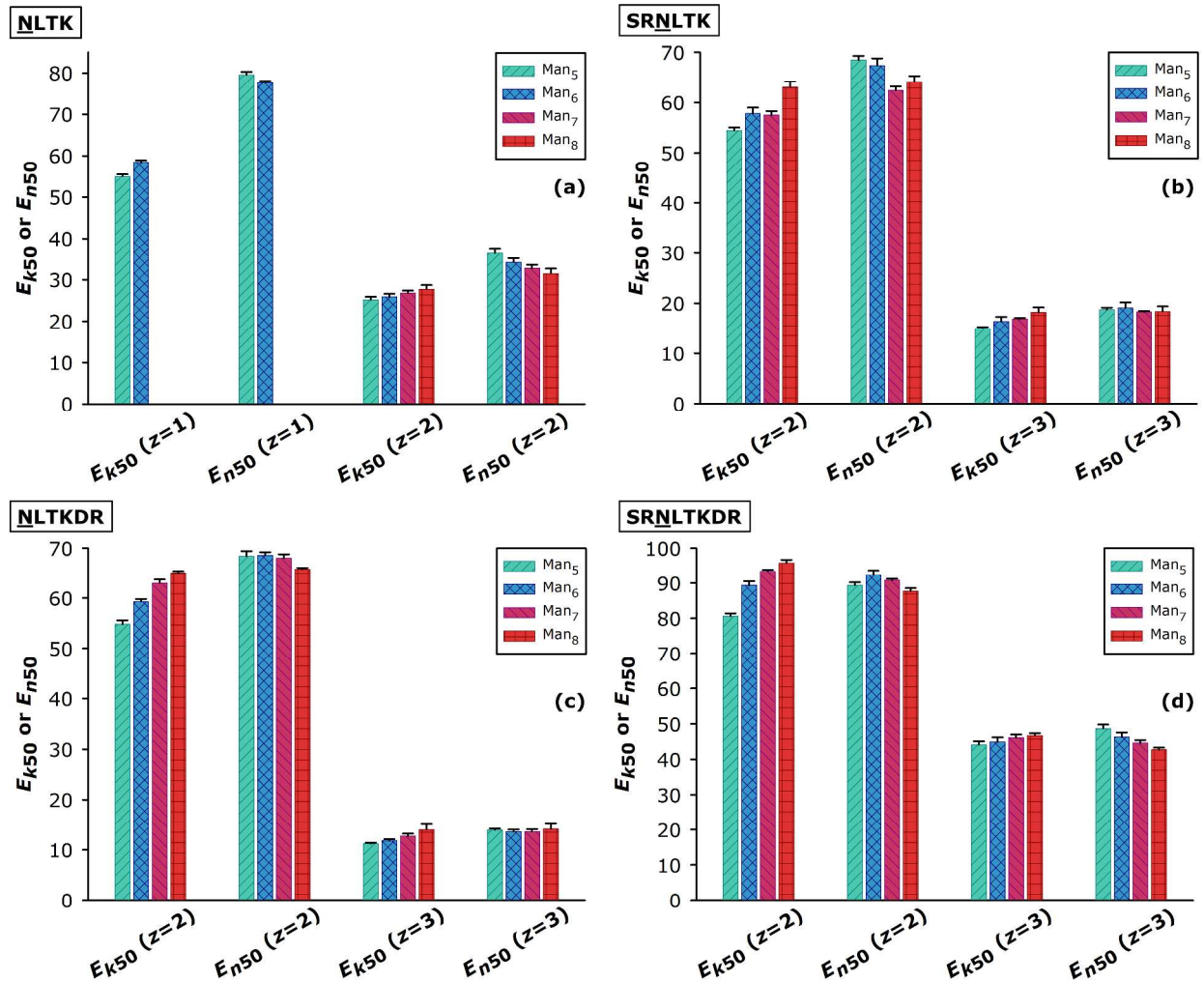


Figure 3. Precursor ion survival energies (expressed as both E_{k50} and E_{n50} values) for glycopeptides with the peptide sequences NLTK **(a)**, SRNLTK **(b)**, NLTKDR **(c)**, and SRNLTKDR **(d)**, harboring N-linked glycans with the compositions GlcNAc₂Man₅, GlcNAc₂Man₆, GlcNAc₂Man₇, and GlcNAc₂Man₈. Two charge states were considered in each case: $z = 1$ and $z = 2$ in **(a)**; $z = 2$ and $z = 3$ in **(b - d)**. Error bars represent the standard deviation of four replicate determinations arising from separate acquisitions. Data for the

[NLTK + GlcNAc₂Man₇ + H]⁺ and [NLTK + GlcNAc₂Man₈ + H]⁺ ions are not shown in **(a)** due to insufficient ion signal for reproducible study.

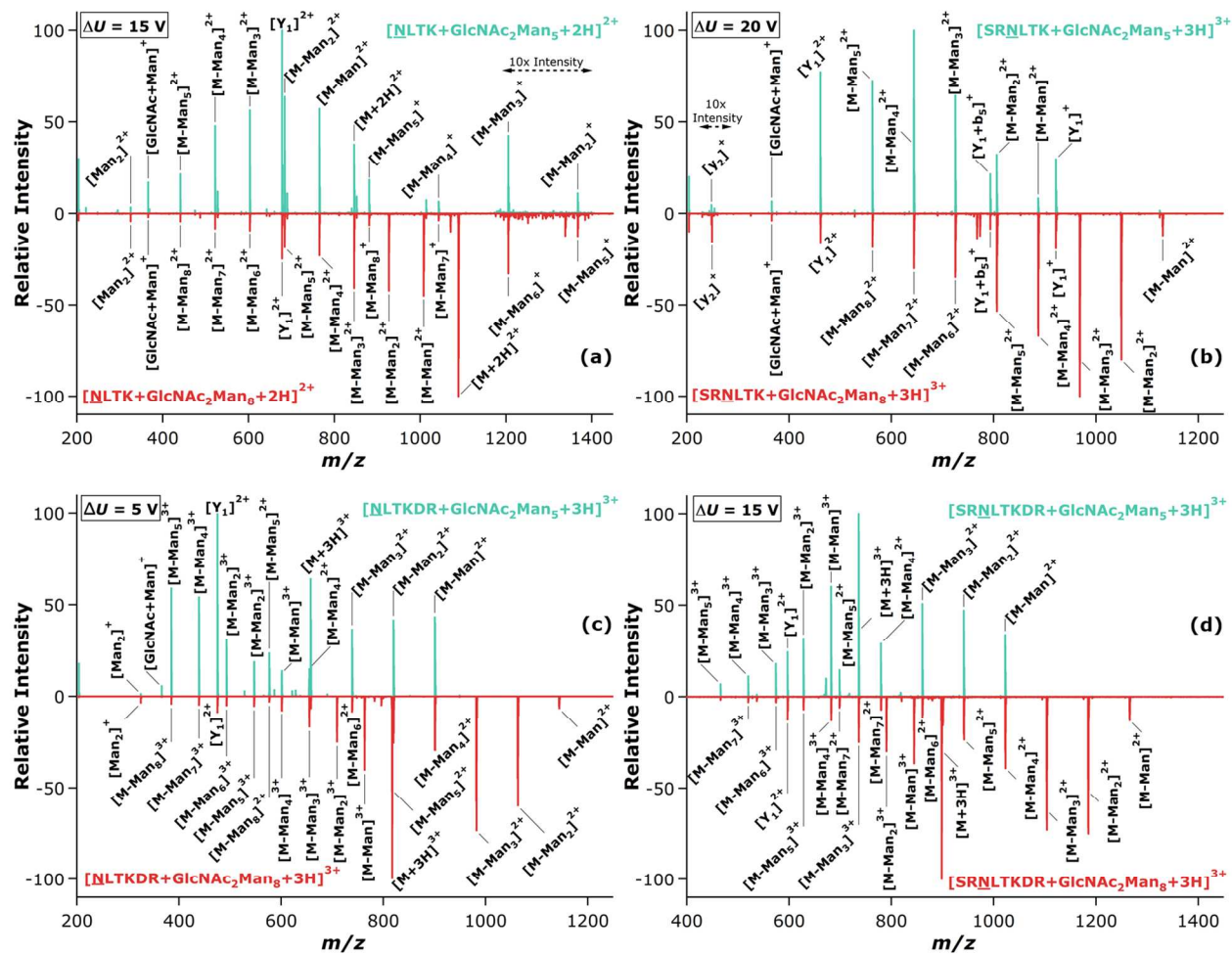


Figure 4. CID spectra for glycopeptides with the peptide sequences NLTK **(a)**, SRNLTK **(b)**, NLTKDR **(c)**, and SRNLTKDR **(d)**, harboring N-linked glycans with the compositions GlcNAc₂Man₅ (top, upright traces) and GlcNAc₂Man₈ (bottom, inverse traces). For each comparison, the same ΔU (indicated in each inset) was applied to acquire the two fragmentation spectra.

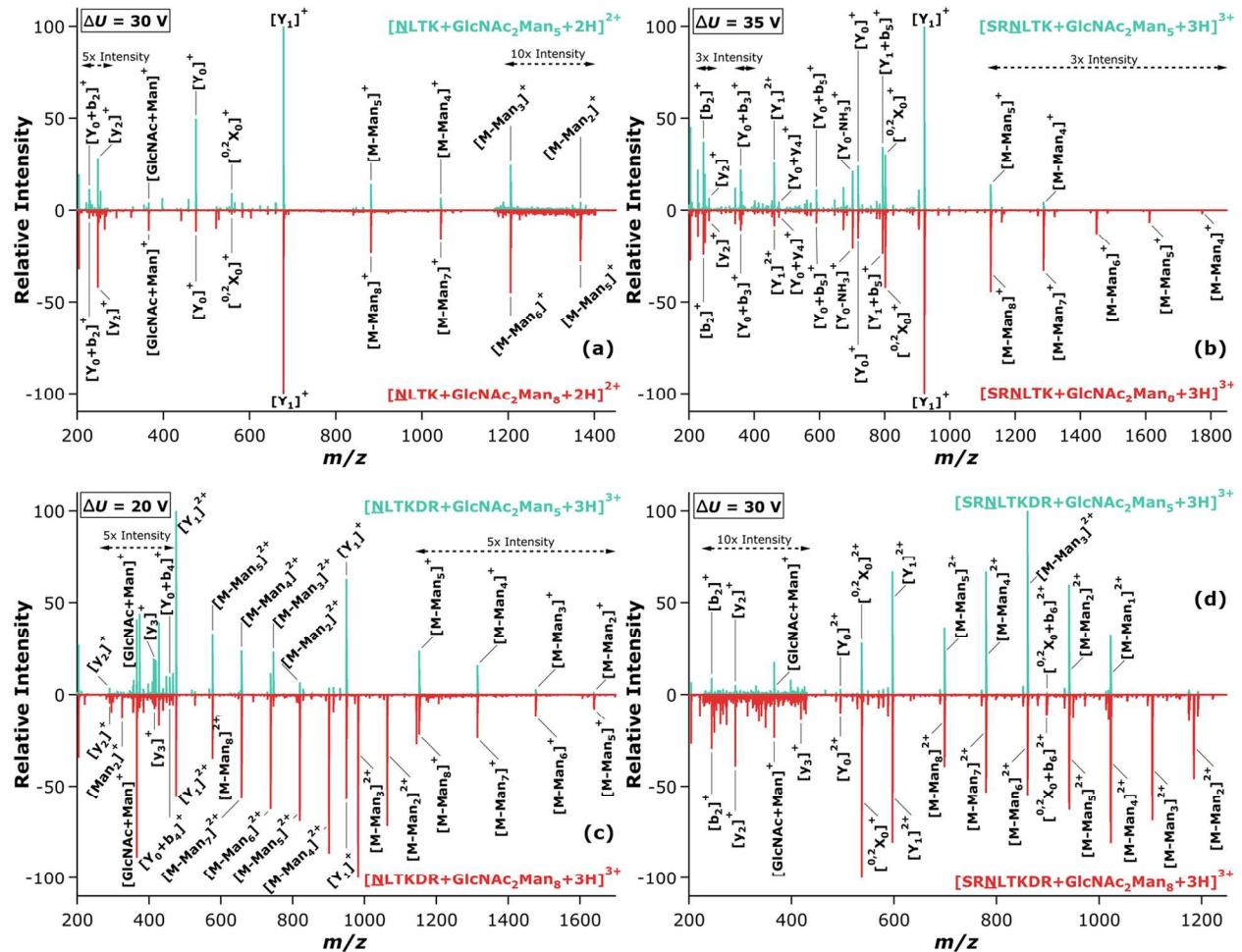
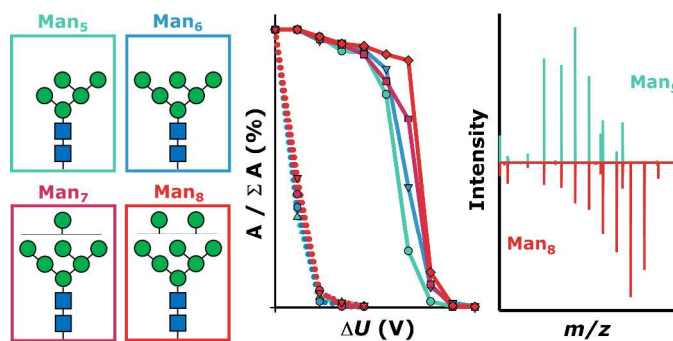


Figure 5. CID spectra for glycopeptides with the peptide sequences NLTK (**a**), SRNLTK (**b**), NLTKDR (**c**), and SRNLTKDR (**d**), harboring N-linked glycans with the compositions GlcNAc₂Man₅ (top, upright traces) and GlcNAc₂Man₈ (bottom, inverse traces). For each comparison, the same ΔU (indicated in each inset) was applied to acquire the two fragmentation spectra. The collision energies were selected such that the applied ΔU values were 15 V greater than those shown in **Figure 4**.

GRAPHICAL ABSTRACT**TEXTUAL ABSTRACT**

This work demonstrates that optimum conditions for CID MS/MS of high mannose N-glycopeptides is relatively insensitive to the glycan composition.